

Magnetically Induced Termination of Giant Planet Formation

A.J. Cridland^{1*}

¹*Leiden Observatory, Leiden University, 2300 RA Leiden, the Netherlands*

14 September 2018

ABSTRACT

Here a physical model for terminating giant planet formation is outlined and compared to other methods of late stage giant planet formation. As pointed out by Batygin (2018), gas accreting into a gap and onto the planet will encounter the planet’s dynamo-generated magnetic field. The planetary magnetic field produces an effective cross section through which gas is accreted. Gas outside this cross section is recycled back into the protoplanetary disk, hence only a fraction of mass that is accreted into the gap remains bound to the planet. This cross section inversely scales with the planetary mass, which naturally leads to stalled planetary growth late in the formation process. We will see that this method naturally leads to Jupiter-massed planets and does not invoke any artificial truncation of gas accretion as has been done in some previous population synthesis models. The mass accretion rate depends on the radius of the growing planet after the gap has opened, and we will see that so-called ‘hot start’ planets tend to end up more massive than ‘cold start’ planets. When combined with population synthesis models this result could show observable signatures of cold-vs-hot start planets in the population of exoplanets.

Key words: protoplanetary discs, planetary atmospheres

1 INTRODUCTION

While giant planet formation on the whole is a relatively slow process (\sim few Myr) in the classical core accretion scenario its final stage of gas accretion occurs very quickly (Polack et al. 1996). Once begun, a giant planet can accrete a Jupiter mass of gas on timescales as low as $\sim 10^4$ yr. With such small timescales, it is unlikely that the final stage of a protoplanetary disk - its evaporation - can be the sole terminator of planet formation.

All large planets evolve through a phase in which they open a gap in their protoplanetary disk. When the planet is sufficiently massive its gravitational influence can exceed the viscous forces in the disk, opening the gap (Lin & Papaloizou 1986; Bryden et al. 1999), and decoupling the planet from the surrounding gas disk. When this happens, the physical processes that govern planet migration (ie. Type-II migration), and gas accretion change. It has been proposed that the termination of gas accretion should be linked to this decoupled phase of planet formation, however hydrodynamic simulations (see for ex. Szulágyi et al. (2014, 2016)) have shown that gas continues to flow into the gap of Jupiter massed planets. Hence simply opening a gap is insufficient to explain the final masses of planets.

Morbidelli et al. (2014) discuss this ‘terminal mass problem’, arguing that there is no obvious reason why the process of gas accretion should stop. In other words we lack a complete physical picture to explain the final mass of Jupiter, Saturn, and the observed exoplanet population.

In this paper, we will explore a simple physical picture for the termination of gas accretion on giant planets based on the recent work of Batygin (2018). This picture begins with the idea that gas accretion through a gap is predominately done through vertical circulation of gas from regions of the disk above the midplane (Szulágyi et al. 2014; Morbidelli et al. 2014). As it falls towards the planet the gas encounters a magnetic field that is being generated by a magnetic dynamo in the convective layer of the forming planet’s interior. Within the magnetosphere (defined in §3) magnetic effects dominates the gas dynamics over gravity, and gas tends to flow along field lines rather than free fall to the midplane. Hence gas can be funnelled away from the planet into the circumplanetary disk if it lands on the far side of the critical magnetic field line’s crest. Once in the circumplanetary disk the gas is recycled back into the protoplanetary disk as it transfers angular momentum away from the planet.

In this work we will see how this simple physical picture can lead to stalled planetary growth. In §2 we outline the rate of gas flow into the gap in both a 1D and 3D picture. In §3 the physical model of Batygin (2018) is summarized and

* E-mail: cridland@strw.leidenuniv.nl

we derive a rate of gas accretion onto the planet. The planet formation model that is used to test the late stage effect of this new accretion rate is outlined in §4. The results of the magnetically terminated gas accretion model is presented in §5. We summarize and conclude in §6.

2 THE RATE OF GAS FLOW INTO A PLANETARY GAP

In a one-dimensional sense, once a gap has opened the growth rate of a planet is limited by the rate that gas can be delivered to the gap edge. Hence it follows that the maximum gas accretion rate onto the planet is related to the global mass accretion rate through the disk (see for example Ida & Lin (2004); Mordasini et al. (2015)). Accretion disks tend to relax to a quasi-steady state (Papaloizou & Terquem 1999) with a mass accretion rate of (Alibert et al. 2005):

$$\dot{M}_{1D} = 3\pi\nu\Sigma_g, \quad (1)$$

where $\nu = \alpha H^2 \Omega$ is the gas viscosity in the standard α -disk prescription (Shakura & Sunyaev 1973) (with $\alpha = 0.002$ in our disk model, discussed below), Σ_g is the gas surface density, H is the scale height of the gas, and Ω is the Keplerian frequency. 2D numerical simulations (ie. Bryden et al. (1999)) have shown that material continues to flow through the gap, with some fraction of it being delivered to the planet. Hence in this simple picture, the rate at which material is delivered can be no quicker than in eq. 1. This provides a very natural, albeit slow, method of terminating gas accretion because the mass flux through a disk preferentially drops as the disk ages (see for ex. Alessi et al. (2017)).

This picture becomes more complicated when considering the flow of material in 3D. As pointed out by Morbidelli et al. (2014), the typical 1D treatment of material flowing into the gap (ie. eq. 1) ignores an important effect coming from the disk's vertical structure. In particular, if the disk is in hydrostatic equilibrium in the vertical direction, its gas density has the same radial dependency at all heights. However the planet's gravitational influence drops with height above the midplane, which allows material to cross the traditional boundary of the gap more easily from a height $z > 0$ than it can from the midplane (Morbidelli et al. 2014).

Once the gas enters the gap it immediately loses its pressure support and rapidly falls to the midplane where it is either accreted by the planet, or filtered back into the disk. The gas that is filtered back into the disk increases the density along the disk midplane, which forces gas towards the disk surface to reinstate hydrostatic equilibrium (Morbidelli et al. 2014). This recycles material back up to heights that can again flow into the gap.

Morbidelli et al. (2014) derive a faster rate of material delivery into the gap than in eq. 1 because the circulation described above evolves on a dynamical timescale rather than the viscous timescale. In this case, the mass accretion rate into the gap at a disk radius r is:

$$\dot{M}_{3D} = 2\pi r [\alpha(H/r)r\Omega] 4\Sigma_g,$$

where the terms in the square bracket are the radial speed of the gas through the disk midplane, and the extra factor of

4 that precedes Σ_g accounts for the inner and outer edges of the gap, and the top and bottom surface layers of the disk.

We rewrite their expression to look more similar to eq. 1:

$$\dot{M}_{3D} = 8\pi\nu(r/H)\Sigma_g, \quad (2)$$

using the definition of viscosity. Notice that the mass accretion rate depends on the inverse of the disk scale height ratio (H/r), which has a typical value of 5%, hence $\dot{M}_{3D}/\dot{M}_{1D} \sim 50$.

As already noted, not all of the material that is accreted into the gap ends up on the planet. In the 1D case gas entering the gap is rotationally supported, entering into a circumplanetary disk. In which case the rate of gas accretion onto the planet is limited by the accretion rate through the circumplanetary disk. This can in principle result in a different accretion rate onto the planet because the circumplanetary disk has a different physical structure (and hence different mass accretion rate) than the surrounding protoplanetary disk.

Due to vertical circulation in the 3D case gas falls vertically towards the planet. Any gas that is not accreted onto the planet flows into a circumplanetary disk and is recycled back into the protoplanetary disk. This physical picture contains two important differences to the 1D model: (1) the net direction of material flow through the circumplanetary disk (outward) is different here than in the 1D case (inward). And (2) while in the 1D case the accretion rate onto the planet is limited by the efficiency that gas can accrete through the circumplanetary disk, the limiting factor in the 3D case depends more on the geometry of the accretion.

Neither of these methods explicitly predict what percentage of the material is accreted onto the planet, and often this is modelled using some 'efficiency' factor, such that:

$$\dot{M}_p = \dot{M}\epsilon, \quad (3)$$

where \dot{M} is the mass accretion rate into the gap (either \dot{M}_{1D} or \dot{M}_{3D}), and $\epsilon < 1$. In the 1D case ϵ represents a parameterization of the viscosity in the circumplanetary disk, while in the 3D case we propose that it is a geometric factor describing the fraction of gas that can accrete onto the planet.

Particular values of ϵ vary between different works: for example Morbidelli et al. (2014) suggest $\epsilon = 0.5$ for their fiducial setup, while Bitsch et al. (2015) used $\epsilon = 0.8$ in their formation models. For both the 1D and 3D gas accretion models, planetary growth is eventually terminated because the surface density of the surrounding gas drops as the disk evolves. However this rate can remain high enough in typical disks to over produce very massive planets within 1 AU, unless their growth is artificially truncated.

Before exploring a more complicated model, we note that a current method of limiting the mass of a planet is by setting a maximum planetary mass:

$$M_{max} = f_{max} M_{gap}, \quad (4)$$

above which the gas accretion is artificially stopped. This parameterization is related to the gap opening mass (M_{gap}), which at least relates this method to the expectation that accretion termination is related to the planet opening a gap in the disk. This method has been used in both population synthesis models (Hasegawa & Pudritz 2013; Alessi & Pudritz 2018), as well as in 'end-to-end' planet formation mod-

els (Cridland et al. 2016, 2017) to simplify the final stages of planet accretion by ignoring the physical processes responsible for terminating planetary growth. In population synthesis models f_{max} is randomly selected from a range of 1-500, which given that $M_{gap} \lesssim 10 M_{\oplus}$ results in a population of giant planets with a mass range of $\sim 10 M_{\oplus} - 15 M_J$. While it is useful for statistical studies, f_{max} has little connection to the underlying physics which result in the termination of gas accretion.

3 MAGNETICALLY LIMITED GAS ACCRETION

From three dimensional hydrodynamic simulations of gas accretion through a gap, Szulágyi et al. (2014) showed that the bulk of gas accreted into the gap (90%) did so by falling vertically from heights above the midplane of the disk. In the absence of planetary accretion this gas formed a circumplanetary disk and then returned to the surrounding protoplanetary disk.

With the addition of a magnetic field, there is a characteristic radius (R_t , see below) within which magnetic effects will alter the flow of the weakly ionized gas. As illustrated by Batygin (2018), within this radius the flow is confined to the magnetic field lines, entering into a force-free configuration ($\mathbf{v} \times \mathbf{B} \rightarrow 0$), rather than free-falling. Hence when gas falls on the critical field line it flows onto the planet if it lands on the planet side of the line's apex. Otherwise it is deflected away from the planet to join the circumplanetary disk.

Given a flow of material into the gap, \dot{M} , the characteristic radius within which magnetic effects dominate the dynamics of the gas is (Batygin 2018):

$$R_t = \left(\frac{\pi^2}{2\mu_0} \frac{\mathcal{M}^4}{GM_p \dot{M}^2} \right)^{1/7}$$

$$R_t = R_0 \left(\frac{M_p}{M_{\oplus}} \right)^{-1/7} \left(\frac{\dot{M}}{M_{\oplus}/yr} \right)^{-2/7}, \quad (5)$$

where $R_0 = (\pi^2/2\mu_0 \mathcal{M}^4/GM_{\oplus}^2/yr)^{1/7}$ has units of length, and $\mathcal{M} = BR_p^3$ is the magnetic moment of an (assumed) magnetic dipole. We follow Batygin (2018) in setting the strength of the magnetic field as $B = 500$ Gauss which is about two orders of magnitude stronger than Jupiter's magnetic field today, but lower than the typical field strength driven for ~ 1000 K brown dwarfs. We select a radius of the young planet $R_p = 2R_J$ as it is a nominal size for young, self-luminous planets with masses $\gtrsim 100 M_{\oplus}$ reported by Mordasini et al. (2015). We assume that both of these quantities remain constant throughout the latter stages of planet formation (see below).

Neither of these physical quantities are well constrained by observations, and their evolution during the phase of rapid gas accretion is not known *a priori* in our model. As argued in Batygin (2018), a sub-kilo Gauss magnetic field is consistent with our understanding of magnetic dynamo theory for young, self-luminous, Jupiter massed planets. Furthermore, as illustrated by Christensen et al. (2009) a sub-kilo Gauss magnetic field is a good interpolation for what we understand of the geo-dynamo and solar-dynamo.

The source of the magnetic field comes from the convective cells which transports heat through the internal structure of the gas giant (Christensen et al. 2009). Assuming the field is in equipartition with the kinetic energy of the convective cell, the strength of the magnetic field should roughly scale as $B \propto \sqrt{\rho v_{conv}^2}$ (Christensen et al. 2009; Batygin 2018), where ρ is the average density of the convecting region, and v_{conv} is the convection speed. This speed is related to the rate of energy transport through convection, and hence on the internal energy flux of the planet.

While the total luminosity of the planet greatly increases during gas accretion (Mordasini 2013) this energy largely comes from the release of gravitational energy by the accreting gaseous envelope. Some of this energy is absorbed by the planet, and hence the rate of convection can in principle change as the planet grows. The amount of energy that is absorbed by the planet differentiates two formation scenarios - the so called 'hot' and 'cold' start models. In the 'hot start' model some of the accretion luminosity is absorbed by the planet, increases its internal temperature. While in the 'cold start' model the majority of the accretion luminosity is radiated away. Assuming that the magnetic field remains in equipartition with the convection cells, these two scenarios may generate different strengths and evolutions of the magnetic field. However for simplicity we keep the magnetic field constant.

Mordasini (2013) computes a self-consistent model for the internal structure of accreting gas giants. Among the planetary properties that is computed, he shows the evolution of the planet's outer radius in his Fig. 1. When a planet opens its gap, and detaches from the surrounding disk, it rapidly reduces its radius from approximately the Hill radius (R_H , see below) to a few Jupiter radii (see Fig. 1 in Mordasini (2013)), depending on the entropy of the planet when the gap is opened. For a 'hot start' planet (high entropy), the outer radius evolves to between 3-4 R_J for the remainder of its gas accretion. For a 'cold start' planet (low entropy), its radius evolves to $\sim 1.5 R_J$ after the gap is opened. Hence our choice of 2 R_J represents an average value of these two scenarios. After the gap opens, the planetary radius shows little evolution (Mordasini 2013) hence keeping it constant during the latter stages of planet formation seems reasonable.

Because of its contrasting formation scenarios we will also compute the formation of a 'cold start' planet with $R = 1.5 R_J$ and a 'hot start' planet with $R = 3 R_J$.

Within a distance of R_t from the planet the dynamics of the gas is dominated by magnetic effects, confining the gas to the field lines rather than allowing it to free fall to the midplane. This confinement requires low gas resistivity, such that the magnetic Reynolds number (Rm) is larger than one. This can most easily be attained at temperatures > 1000 K when alkali metals are thermally ionized. Such gas temperatures are readily produced around young forming planets in hydrodynamic simulations (see for example Szulágyi et al. (2016)). Additionally when a gap is opened in the disk, the gas can become more susceptible to X-ray ionization as argued by Tan & Chatterjee (2013), further raising the Reynolds number. Here we generally assume that the incoming gas is sufficiently ionized such that $Rm \gg 1$ and it remains confined to the magnetic fields.

Hence as the gas falls on the critical field line it flows

onto the planet if it lands planetward of the field line's crest, while otherwise it flows along the field line onto the circumplanetary disk. Once in the disk the gas flows back into the surrounding protoplanetary disk as it carries angular momentum away from the planet (Batygin 2018). This naturally sets a vertical cross section that will limit the rate of mass accretion on the planet, which for a dipole field is roughly $A_{mag} \sim \pi R_t^2 / 3^{3/4}$ (Batygin 2018). Comparing this cross section to the total accreting area around the planet allows us to derive an accretion efficiency (ϵ).

We will assume that the total accretion area is the cross section of the circumplanetary disk. Szulágyi et al. (2014) run numerical simulations of gas accretion onto giant planets through a gap. They report radii of the resulting circumplanetary disks which range between $\sim 0.28 - 0.75$ Hill radii ($R_H = a(M_p/3M_*)^{1/3}$) depending on their (numerical) viscosity. The edge of the circumplanetary disk connects to the protoplanetary disk at the gap edge. If we assume that the material accreting into the gap falls homogeneously across the planet-circumplanetary disk system then the accretion efficiency (ϵ) would be the ratio of A_{mag} and the cross section of the circumplanetary disk: $A_{grav} = \pi R_H^2 / 4$ - where we choose a nominal circumplanetary disk radius of $0.5 R_H$. Hence:

$$\begin{aligned} \epsilon &= A_{mag} / A_{grav} \\ &= \frac{4R_t^2}{3^{3/4} R_H^2} \\ &= \frac{4}{3^{3/4}} \left(\frac{R_0}{R_H} \right)^2 \left(\frac{M_p}{M_\oplus} \right)^{-2/7} \left(\frac{\dot{M}}{M_\oplus / yr} \right)^{-4/7}. \end{aligned} \quad (6)$$

Noting again that \dot{M} is the mass accretion rate into the gap, we combine eqs. 3 and 6:

$$\frac{\dot{M}_{p,Mag}}{M_\oplus / yr} = \frac{4}{3^{3/4}} \left(\frac{R_0}{R_H} \right)^2 \left(\frac{M_p}{M_\oplus} \right)^{-2/7} \left(\frac{\dot{M}}{M_\oplus / yr} \right)^{3/7}. \quad (7)$$

Hence the gas accretion rate is stifled as the planet grows. There are two mass dependent terms in eq. 7, recalling that $R_H \propto M_p^{1/3}$, the overall mass dependence of the accretion rate is: $\dot{M}_{p,Mag} \propto M^{-20/21}$.

We can interpret eq. 7 in two ways. First as the planetary mass grows, the region where the magnetic force is relevant to the gas dynamics shrinks, hence so too does the planets accretion cross section. Second the physical size of the gap grows with the planetary mass. Assuming that the mass accretes homogeneously across the total disk cross section, the quantity of mass available within R_t also naturally shrinks.

The general picture is as follows: the gas that falls towards the planet outside of R_t has too much angular momentum relative the planet to accrete directly, and falls to the circumplanetary disk. As argued by Batygin (2018) the disk is carrying rotational angular momentum away from the planet, transporting material away from planet back to the protoplanetary disk (as required by Morbidelli et al. (2014)). Gas that falls within R_t feels the effect of the magnetic field, and will accrete onto the planet along the magnetic field lines as long as it lands within the cross section defined by A_{mag} . Otherwise it flows along the field line to the circumplanetary disk, away from the planet. As the planet grows its gravitational influence grows which shrinks the cross section

within which gas can continue to accrete onto the planet - eventually stifling further growth.

4 CORE ACCRETION MODEL

To test the effects of this new gas accretion terminator we modify the final stages of the planet formation model outlined in Alessi et al. (2017), and Cridland et al. (2017). Those models assumed the standard planetesimal accretion scheme (Kokubo & Ida 2002; Ida & Lin 2004) with a planet-trapping model of planet migration (Hasegawa & Pudritz 2011) to build the initial $\sim 10 M_\oplus$ planetary core. When the growing core is sufficiently massive it begins a phase of gas accretion that is first limited by the Kelvin-Helmholtz time (Ikoma et al. 2000):

$$t_{KH} = 10^c yr \left(\frac{M_p}{M_\oplus} \right)^{-d}, \quad (8)$$

such that:

$$\dot{M}_{p,KH} = \frac{M_p}{t_{KH}}, \quad (9)$$

where the parameters c and d depend on the opacity of the accreting planetary envelope κ_{env} (Ikoma et al. 2000; Miguel & Brunini 2008; Mordasini et al. 2014; Alessi & Pudritz 2018). Recently, Alessi & Pudritz (2018) tested fitted functions for both $c(\kappa_{env})$ and $d(\kappa_{env})$ based on the work of Mordasini et al. (2014) using population synthesis models and found a preferred value of $\kappa_{env} = 0.001 \text{ cm}^2 \text{ g}^{-1}$ best reproduced the population of known exoplanets. Using their preferred values we use: $c = 7.7$ and $d = 2.0$.

Eventually, the growing planet becomes sufficiently massive that its gravitational influence exceeds the fluid dynamics that otherwise govern the structure of the disk. This is characterized by either the gravitational torque of the planet on the surrounding material exceeding the disk viscosity torque, or the planet's gravitational influence (R_H) exceeding the typical length scale of the gas pressure (H). Once one of these requirements are met we say that the planet has opened a gap. This has a characteristic gap opening mass of (Matsumura & Pudritz 2006):

$$M_{gap} = M_* \min \left(3h^3, \sqrt{40\alpha h^5} \right), \quad (10)$$

where $h = H/r$ is the disk scale height ratio. The first term represents the mass required for $R_H = H$, while the second term represents the mass required for the planet's gravitational torque to exceed the disk viscous torques.

Once the gap is open, the magnetically limiting gas accretion term from eq. 7 can begin to impact the flow rate of gas onto the planet. However if the rate exceeds $\dot{M}_{p,KH}$ then the gas can not lose its excess gravitational potential energy fast enough to fully accrete onto the planet. Hence the actual accretion rate will be which ever one is smaller:

$$\dot{M}_p = \min \left(\dot{M}_{p,KH}, \dot{M}_{p,Mag} \right). \quad (11)$$

The method that builds the original solid core on which gas is accreted remains a debated topic. The classical core accretion model (now known as 'planetesimal accretion', ie. Pollack et al. (1996), Kokubo & Ida (2002), and Ida & Lin (2004)) posits that the proto-planetary core is built from the successive collisions of 10-100 km planetesimals onto

$\sim 0.01 - 0.1 M_{\oplus}$ embryo. A potentially catastrophic issue with this model is that its typical timescale ($\sim 10^5$ yr) is about an order of magnitude longer than the Type-I migration rate for planets with masses of $\sim M_{\oplus}$ (Masset et al. 2006). Hence planets should be lost through disk-planet interactions before they could accrete to masses large enough to accrete gas (few M_{\oplus}).

Two models have been suggested to remedy the ‘Type-I migration problem’: planet trapping, and pebble accretion. The former slows the Type-I migration rate through disk inhomogeneities which lead to positions in the disk where the net torque on the planet goes to zero - often called ‘planet traps’ (or convergence zones, see the review by Pudritz et al. (2018)). The latter remedy assumes that solid accretion is dominated by cm-sized particles, and hence accrete at a much faster rate because they are less susceptible to gravitational scattering than planetesimals (see the review by Morbidelli (2018)).

While the details of core accretion are less important to our current discussion (in as much as we require a core to form and accrete gas) it is worth noting that the rate of solid core accretion could position the proto-planet in such a way that it does not accrete an excessive amount of gas before the gas disk evaporates. In this way we can view super-Earth planets as ‘failed’ Jupiter cores, that either did not have enough time to accrete a significant gaseous envelope, or grew in an excessively low density environment to undergo runaway gas accretion.

The planets undergoing magnetically terminated gas accretion have all opened a gap (by construction) and hence are not subject to Type-I migration. Instead they enter into the second stage of planet migration: Type-II. In Type-II migration the planet acts as an intermediary for the global angular momentum transport in the disk, and shrinks its orbital radius on the viscous timescale $t_{\nu} \sim \nu/r_p^2$, such that:

$$\frac{1}{r_p} \frac{dr_p}{dt} = -\frac{\nu}{r_p^2}. \quad (12)$$

This rate persists until the planetary mass exceeds the mass of the disk gas inward of the planet $M_{crit} \sim \pi \Sigma r_p^2$. In this regime the migration rate is said to be limited by the planet’s own inertia:

$$\frac{1}{r_p} \frac{dr_p}{dt} = -\frac{\nu}{r_p^2} (1 + M_p/M_{crit})^{-1}. \quad (13)$$

In what follows we use the standard planetesimal accretion scenario for a planetary embryo trapped at the water ice line (see Cridland et al. (2016) and Alessi & Pudritz (2018) for technical details).

5 RESULTS

To show the effect of the magnetically terminated gas (MTG, eq. 7) accretion rate we compare it to the 1D (eq. 1) and 3D (eq. 2) gap accretion rates as discussed in §2. Following Bitsch et al. (2015) and Morbidelli et al. (2014) we assume that the efficiency (ϵ) is 0.8 and 0.5 for the 1D and 3D accretion rates respectively. We run our planet formation model over 7 Myr of evolution, which would constitute a very old disk, at least one standard deviation outside of the mean age of protoplanetary disks (see Alessi & Pudritz (2018) for a theoretical distribution of disk ages). Where

needed, we impose a maximum mass using $f_{max} = 100$ for all models other than MTG.

We build planets in the simple evolving disk model reported by Eistrup et al. (2017). The model fits a radial power-law to the temperature and surface density profiles computed by Alibert et al. (2013). As the model evolves the gas cools and the surface density drops as one would expect from a viscously accreting protoplanetary disk. In that way, this model reflects the way in which the lowering mass accretion rate through the disk can terminate the growth of giant planets. In this disk model the mass accretion rate as computed with eq. 1 is only a few $\times 10^{-10} M_{\odot}/\text{yr}$, which is on the low end of the typical mass accretion rates for disks: $10^{-7} - 10^{-10} M_{\odot}/\text{yr}$. To account for the possibility that the mass accretion rate through the disk could be higher, we also test a model where the 1D gap accretion rate is raised by an order of magnitude. Below we call this model the ‘enhanced’ 1D gap model.

For the gap accretion rate (\dot{M}) in eq. 7 we use the 3D accretion rate from eq. 2 because it represents (as we will see) the highest accretion rate we model. This will illustrate the utility of MTG as a method of limiting gas accretion.

5.1 Gas accretion history

In Figure 1 we show different representations of the formation histories of planets growing with the four different accretion models: the magnetically terminated gas model (MTG), the 1D gap model, the enhanced 1D gap model (1D $\times 10$), and the 3D gap model. Each planet begins at the same point in the disk at the same point in the disk history. Each planet undergoes the same early evolution, and hence they all open a gap in their disk at the same point in time, denoted by the black dashed line. The main differences between each planet is when they break away from the unstable gas accretion phase (shortly after gap opening), and the rate at which material is accreted at later times. Below we summarize some key points.

In Figures 1(a) and 1(b) we show the temporal evolution of the planetary mass accretion rate and planet mass respectively. In both the enhanced 1D and 3D accretion models the planet reaches a maximum mass (eq. 4) that was set with $f_{max} = 100$. They are nearly indistinguishable in these figures, as they follow similar accretion histories. This is important to note because in population synthesis models that either have high disk masses or have planets that grow early in the disk lifetime, the choice of f_{max} becomes the key parameter in determining the final mass of the planet. Conversely, in the 1D gap accretion model the accretion rate is so low that the planet never approaches the maximum mass, hence planets forming in lower mass disks or later in the disk lifetime are less sensitive to the choice of f_{max} .

The planet growing with the MTG accretion rate coincidentally grew to a mass that was similar to the maximum mass set by f_{max} . However it took the full 7 Myr of growth to do so. This implies that the disk lifetime becomes more important in determining the final mass of the planet than in the accretion models that were limited by f_{max} .

In Figure 1(c) we show an accretion timescale which is effectively a ‘mass-doubling time’, defined as the ratio between a planet’s current mass and its current mass accretion rate. It becomes clear why the MTG accretion model is an

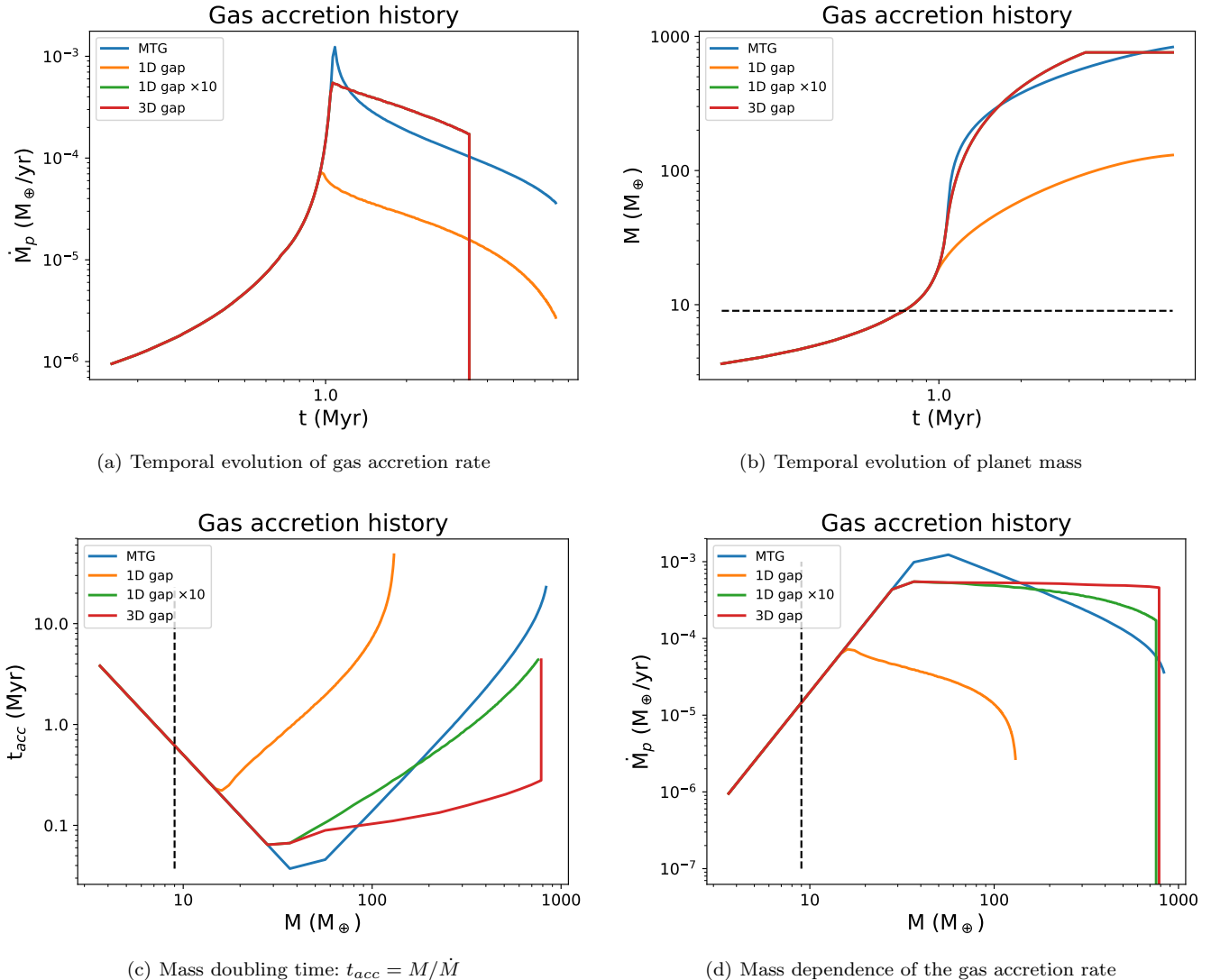


Figure 1. Evolution of the gas accretion history. For the magnetically terminated gas accretion (MTG, eq. 7), 1D disk accretion into the gap (eq. 1), and the 3D gap accretion as prescribed by Morbidelli et al. (2014) (eq. 2). We up the rate of the 1D disk accretion by a an order of magnitude to account for the possibility that gas accretion into the gap is enhanced by the generation of gravitational instabilities near the gap edge. For the 1D and 3D accretion rates we assumed static efficiencies of 0.8 and 0.5 respectively. In each of subfigures, the black dashed line denotes the point where the planet opens a gap.

effective way of limiting gas accretion while still allowing for planetary growth up to Jupiter mass planets. Namely that the mass doubling time for a $\sim 100 M_\oplus$ object is ~ 0.2 Myr, but rises rapidly as the planet approaches a Jupiter mass. Meanwhile the enhanced 1D and 3D models both have mass doubling times of ~ 0.1 Myr at the same mass but rise slower than the MTG model, explaining their need for setting a maximum mass. The 1D model has a mass doubling time closer to ~ 10 Myr at $\sim 100 M_\oplus$ resulting in its smaller final mass.

In Figure 1(d) we show the mass dependence of the planetary gas accretion rate for each of the models. Here we see the important feature of the MTG accretion model: as the planet grows it becomes harder to gather more material. This is because the planet’s own magnetic field diverts gas into the circumplanetary disk that otherwise would have

been accreted onto the planet, if that gas lands past the crest of the critical magnetic field line. Differing greatly from the other three mass accretion models which only limited gas flow based on the amount of available material flowing towards the planet, MTG is self-regulating.

5.2 Planet formation history

A common way of studying the formation history of synthetic planets is through its planet formation track. This track maps the planet’s evolution through the commonly used mass-semi-major axis diagram.

In Figure 2 we show the formation tracks for the four gas accretion models. Note that while we start the process of solid accretion with an embryo of $0.01 M_\oplus$, we only plot the formation track for masses $> 1 M_\oplus$. The initial step-like

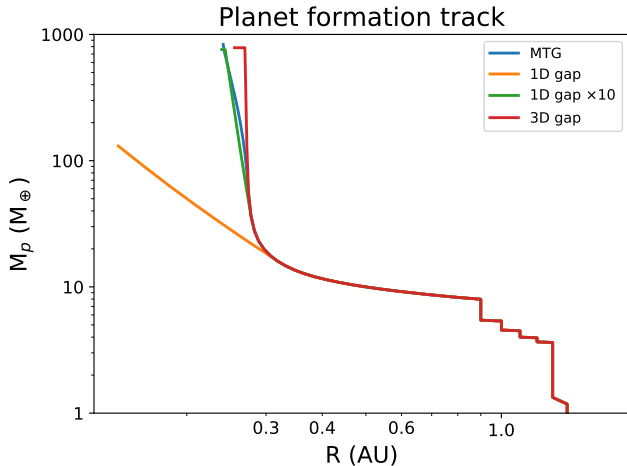


Figure 2. Planet formation tracks for the four accretion models. The step-like evolution of the low mass planet is due the fact that the radial evolution of the planet was dictated by planet-trapping at the water ice line, and hence on the resolution of our disk model. There are instances when the water ice line does not move between timesteps, hence neither does the planet.

growth between $\sim 1 - 10 M_{\oplus}$ is related to our prescribed location of the water ice line (in which the planet is trapped). The location of the water ice line is defined as the most inward radius where water ice becomes more abundant than gaseous water. Its particular location is selected as the disk radius with a gas temperature closest to 170 K, and hence is limited by the spacial resolution of our temperature profiles. There are multiple instances where the water ice line and hence the planet does not move between timesteps. Ultimately this step-like evolution does little to affect the current discussion.

The formation tracks are identical until the planet opens a gap at ~ 0.35 AU where both the migration scheme changes to the classic Type-II migration, and the gas accretion scheme changes to the scenarios outlined above. At this point, since the accretion time scales are all different (see Figure 1(c)) the tracks deviate from each other. The slower accretion rate (1D gap) sees more horizontal evolution than the faster accreters (MTG, 1D gap $\times 10$, 3D gap) because its accretion timescale is equal the viscous timescale - which dictates the rate of inward migration in the Type-II regime. For the fast accreters, once they open a gap their evolution is predominately vertical since their growth rates are faster than the Type-II migration rate. We note that Type-II migration eventually becomes very inefficient as the mass of the planet grows above the total mass of gas within its orbital radius. Hence even when the growth timescale of MTG becomes long (recall Figure 1(b)) its Type-II migration is too low to change the planet’s orbital radius.

The three fast accreters all end their evolution with similar planetary parameters (orbital radius, mass) however as noted earlier, a key difference is that the MTG accretion model doesn’t require an artificial termination of its gas accretion.

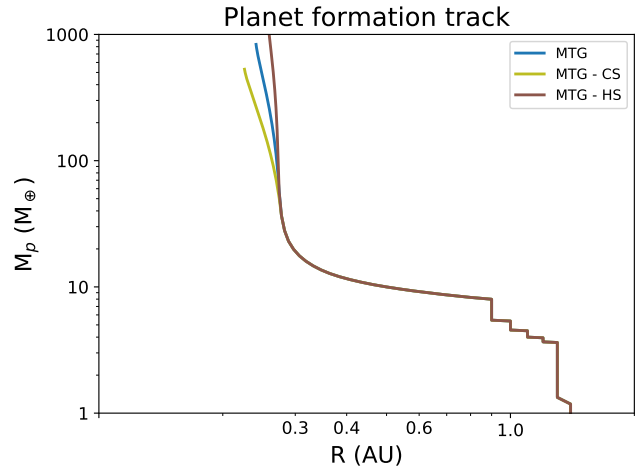


Figure 3. Same as in Figure 2 but comparing the fiducial MTG accretion model to the hot start (HS) and cold start (CS) variants. Here we see by varying the size of the accreting planet we change both the final mass and radius to which it grows. When combined with the assumed age of the disk we can similarly tune the final mass of the planet as with f_{max} .

5.3 Hot vs. Cold starts

The size of the planet when it enters the gap-opening phase of gas accretion is unknown in our model, and has the strongest effect on the resulting formation history of the planet - since $\dot{M}_p \propto R_p^{24/7}$. From Mordasini (2013) the range of these sizes are between 1.5 and $\sim 3 R_J$ depending on whether the planet formed with a so-called cold start (low entropy) or hot start (high entropy) respectively. Here we pick both $R_p = 1.5, 3 R_J$ and re-run the formation.

In Figure 3 we compare the planet formation tracks for the fiducial model ($R_p = 2 R_J$) to the cold (CS) and hot (HS) start variants. The major differences between the three lines are the turn-off point of the track, where MTG accretion begins to take its effect on the growth of the planet, as well as the final mass of the planet. Larger planets have larger magnetic moments, hence they start with a larger magnetic cross section and more efficient accretion (ie. via eq. 6).

Its clear that in MTG accretion the size of the planet after it opens a gap has a strong influence on the late stages of gas accretion, hence it acts like f_{max} from population synthesis models. However unlike f_{max} , the planetary size depends sensitively on the processes that govern the evolution of its internal energy. To compare the two methods, we compute an *effective* $f_{max,e} = M_{final}/M_{gap}$. For the cold start, fiducial, and hot start models we find that $f_{max,e} \sim 160, 244, 465$, which are on the high side of the original range of 1-500 used in population synthesis models. Of course these present calculations were run on an older-than-average disk, and younger disks will result in smaller values of $f_{max,e}$. A tantalizing question arises from this: is there an observable bias in the population of planet towards a hot or cold start? Answering this question is beyond the scope of this paper, and will require a population synthesis model that includes MTG accretion.

6 CONCLUSIONS

Here we have outlined a simple physical model for the termination of gas accretion on a giant planet. This magnetically terminated gas (MTG) accretion model is based on the work of Batygin (2018) who argued that the shrinking magnetosphere (defined by R_t , eq. 5) would naturally limit the available cross section through which gas can accrete onto the planet. Material outside the crest of the critical magnetic field line falls past the planet onto the circumplanetary disk and is filtered back into the surrounding protoplanetary disk. This circulation was described by Morbidelli (2018) and generally results into accretion rates that are between one and two orders of magnitude higher than would be predicted by simple 1D accretion of material through the protoplanetary disk.

Taking the ratio of the magnetic cross section with the cross section of the circumplanetary disk, and assuming that material accretes vertically and homogeneously across the gap results in an efficiency factor ϵ that scales inversely with the mass of the growing planet. This naturally leads to a truncation in planetary growth because the magnetic cross section shrinks as the planet grows. Additionally by construction, the efficiency shrinks with the mass of the planet because the size of the gap increases with planetary mass (through the Hill radius). Hence assuming homogeneous accretion across the gap implies that there is less material available within the magnetic cross section even if R_t was constant.

We are forced to assume (for simplicity in the model) that the magnetic field strength generated by the planetary dynamo as well as the size of the planet remains constant during the final stages of gas accretion, after the gap has opened. There is evidence suggesting that the size of the planet remains constant after gap opening based on formation calculations which include the internal structure of the planet and its evolution (ie. Mordasini (2013)). The dynamo process responsible for the generation of the magnetic field is not constrained by observations, nor is it well understood theoretically. However assuming it is in equipartition with the convective flux in the interior of the planet suggests that it would remain largely unchanged while the planet accretes its outer envelope.

Because the final size of the planet after gap opening is unknown, and depends on the internal processes during formation, we varied the planetary size R_p and tested the resulting formation history of the planet. The range of R_p was determined by the choice of a ‘hot start’ or ‘cold start’ model, which depends on whether the planet has maintained high or low entropy respectively, during its initial accretion. The choice of R_p is effectively similar to the choice of f_{max} in population synthesis models, but is more closely tied to physical processes.

In this framework, the disk lifetime becomes an incredibly important parameter to the population of giant planets. Moving forward, full population synthesis models must be used to test what range of planetary masses are achievable with this method. The key questions are: what is the maximum mass that is attainable using MTG accretion as the limiting model? And given a typical spread in disk lifetimes, can it reproduce the range of planetary masses that we observed?

ACKNOWLEDGEMENTS

Thank you to the anonymous referee for their insightful comments which greatly improved the manuscript. AJC acknowledges financial support from the European Union A-ERC grant 291141 CHEMPLAN, supervised by Ewine F. van Dishoeck. Thanks to Ralph Pudritz and Matthew Alessi for their fruitful discussion during the early stage of this project.

REFERENCES

- Alessi M., Pudritz R. E., 2018, ArXiv e-prints
 Alessi M., Pudritz R. E., Cridland A. J., 2017, MNRAS, 464, 428
 Alibert Y., Carron F., Fortier A., Pfyffer S., Benz W., Mordasini C., Swoboda D., 2013, A&A, 558, A109
 Alibert Y., Mordasini C., Benz W., Winisdoerffer C., 2005, A&A, 434, 343
 Batygin K., 2018, AJ, 155, 178
 Bitsch B., Lambrechts M., Johansen A., 2015, A&A, 582, A112
 Bryden G., Chen X., Lin D. N. C., Nelson R. P., Papaloizou J. C. B., 1999, ApJ, 514, 344
 Christensen U. R., Holzwarth V., Reiners A., 2009, *Nature*, 457, 167
 Cridland A. J., Pudritz R. E., Alessi M., 2016, MNRAS, 461, 3274
 Cridland A. J., Pudritz R. E., Birnstiel T., Cleeves L. I., Bergin E. A., 2017, MNRAS, 469, 3910
 Eistrup C., Walsh C., van Dishoeck E. F., 2017, ArXiv e-prints
 Hasegawa Y., Pudritz R. E., 2011, MNRAS, 417, 1236
 Hasegawa Y., Pudritz R. E., 2013, ApJ, 778, 78
 Ida S., Lin D. N. C., 2004, ApJ, 604, 388
 Ikoma M., Nakazawa K., Emori H., 2000, ApJ, 537, 1013
 Kokubo E., Ida S., 2002, ApJ, 581, 666
 Lin D. N. C., Papaloizou J., 1986, ApJ, 307, 395
 Masset F. S., Morbidelli A., Cridland A., Ferreira J., 2006, ApJ, 642, 478
 Matsumura S., Pudritz R. E., 2006, MNRAS, 365, 572
 Miguel Y., Brunini A., 2008, MNRAS, 387, 463
 Morbidelli A., 2018, ArXiv e-prints
 Morbidelli A., Szulágyi J., Cridland A., Lega E., Bitsch B., Tanigawa T., Kanagawa K., 2014, Icarus, 232, 266
 Mordasini C., 2013, A&A, 558, A113
 Mordasini C., Klahr H., Alibert Y., Miller N., Henning T., 2014, A&A, 566, A141
 Mordasini C., Mollière P., Dittkrist K.-M., Jin S., Alibert Y., 2015, International Journal of Astrobiology, 14, 201
 Papaloizou J. C. B., Terquem C., 1999, ApJ, 521, 823
 Pollack J. B., Hubickyj O., Bodenheimer P., Lissauer J. J., Podolak M., Greenzweig Y., 1996, Icarus, 124, 62
 Pudritz R. E., Cridland A. J., Alessi M., 2018, ArXiv e-prints
 Shakura N. I., Sunyaev R. A., 1973, A&A, 24, 337
 Szulágyi J., Masset F., Lega E., Cridland A., Morbidelli A., Guillot T., 2016, MNRAS, 460, 2853
 Szulágyi J., Morbidelli A., Cridland A., Masset F., 2014, ApJ, 782, 65
 Tan J., Chatterjee S., 2013, in Protostars and Planets VI Posters

This paper has been typeset from a \TeX / \LaTeX file prepared by the author.